Design Study of the Low Energy Part of the CERN Pb Ion Injector

F. Cervellera, G. Fortuna, A. Lombardi, G. Parisi, A. Pisent
INFN, Laboratori Nazionali di Legnaro, I-35020 Legnaro (PD), Italy
G. Amendola, M. Vretenar, M. Weiss
CERN, PS Division, CH-1211 Geneva 23, Switzerland

Abstract

The low energy section of the new CERN lead ion injector which will be built by the Laboratori Nazionali di Legnaro, Italy, includes the part between the ECR ion source and the main Linac. The section is divided into the low energy beam transport, LEBT, operating at 2.5 keV/u, the RFQ, which accelerates up to 250 keV/u and the medium energy part, MEBT, which matches the beam, in 6-D phase space, into the subsequent interdigital accelerator, IH. The charge state used in the design is Pb^{25+}, although the nominal beam delivered by the source is Pb^{28+}. The design methods and the beam transport elements of the section are outlined.

1 INTRODUCTION

The low energy part of the CERN lead ion injector is designed jointly by the Laboratori Nazionali di Legnaro LNL and CERN. The construction itself is of responsibility of LNL.

The low energy part comprises all the elements between the ECR ion source and the interdigital, IH, linear accelerator. This part is conveniently divided into three sections, the low energy beam transport (LEBT), the RFQ and the medium energy beam transport (MEBT).

In the LEBT, the wanted ion type (Pb^{28+}_{208}) is selected and matched into the RFQ. In the RFQ, the energy per nucleon is increased from 2.5 keV/u to 250 keV/u. In the MEBT, finally, the output beam from the RFQ is matched to the IH accelerator in six dimensions.

This paper briefly discusses the deign and the elements of the low energy part of the lead ion injector.
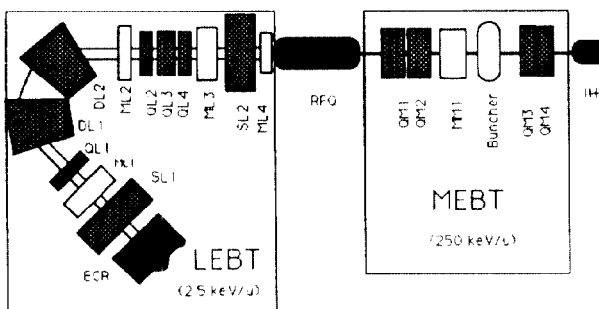
Figure 1: Lay-out of the system (not in scale)

2 SPECIFICATIONS OF THE LOW ENERGY PART

Table 1 summarizes the main specifications given to the complex. From now on in this paper, the quoted emittance and acceptance values are intended to be normalized, total (5 times the r.m.s. value from simulations) and are defined as the product of the semi axes of a right ellipse (area of the ellipse/π).

Table 1: Specifications

LEBT	Energy	2.5 keV/u
	Acceptance	.46 mm mrad
	Resolution $\Delta m/m$	0.003
RFQ	Frequency	101.28 MHz
	Transmission	> 90%
	Max. surface field	22.8 MV/m
	Acceptance	.8 mm mrad
	Longitudinal emittance	< 40°keV/u
MEBT	Energy	250 keV/u
	Acceptance	1 mm mrad

3 LEBT

The central part of the LEBT is a compact spectrometer with a resolution of 0.003. The choice of a bending radius $\rho = .4$ m and a dipole field of .15 T is convenient for the engineering of the magnets. Different configurations have been studied, performing the linear and non linear analysis, with the help of the program GIOS[1]. Non linear aberrations in the dipole magnets are important because (for the given emittance and resolution) the horizontal extension of the beam is nearly equal to the bending radius.

Finally we have selected the same spectrometer design as is used for the LEBT of the new high charge state injector at GSI[2], with two separated 67.5° dipoles; the angles of all pole faces are inclined by 25°, focusing in the vertical plane. The gap height is 80 mm and the pole width 600 mm.

In Fig. 2 are shown the beam envelopes in the LEBT for a typical set of source output parameters (see Table 3)[3].

The advantage of this configuration (two magnets) is the possibility to shim the internal faces of the dipoles so to introduce a sextupole correction; with a curvature of radius 2.68 m of those faces, the second order aberrations of the dipoles can be corrected.

In Table 2 are listed the main matrix elements between
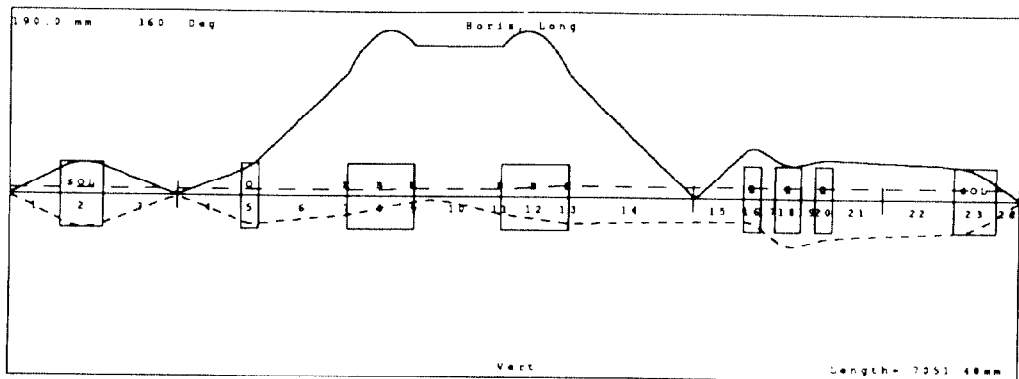
Figure 2: Beam envelopes in the LEBT

the image and the object after correction; x_i is the horizontal beam dimension at the image point. Since the Twiss parameter βs at the object and image points are much smaller than the distance between these points, one can consider the beam waist and the image point locations as coincident (independently from the object spot-size).

Table 2: Matrix elements

Magnification	$\partial x_i/\partial x$	$-.44$
Dispersion	$\partial x_i/\partial(\Delta m/m)$	1.3 m
Aberrations	$\partial x_i/\partial x'$	$+7 \times 10^{-5}$ m
	$\partial^2 x_i/\partial(x'^2)$	-3×10^{-3} m
	$\partial^2 x_i/\partial(x^2)$	-9×10^{-2} m^{-1}
	$\partial^2 x_i/\partial(xx')$	-3×10^{-2}

The resolution, defined as:

$$R = \frac{\partial(\Delta m/m)}{\partial x_i}2x_i = \frac{\partial(\Delta m/m)}{\partial x_i}\frac{\partial x_i}{\partial x}2x \qquad (1)$$

depends on the beam dimensions at object point or, for a given emittance, on the divergence.

In our lay-out the object of the spectrometer is the waist produced by the solenoid SL1; the solenoid and the source can be longitudinally shifted so to obtain the desired spot size at the object point and the desired resolution for a certain range of initial source operating conditions. This gives some flexibility in the choice of the parameters, that will be fixed according to commissioning experience.

After the spectrometer a triplet restores the cylindrical symmetry of the beam, and the solenoid SL2 focuses the beam to match the initial RFQ conditions. Two pairs of steering magnets (horizontal and vertical) are located between the triplet and SL2, so to have the possibility of a position and angle correction at the entrance of the RFQ. Two other steering magnets are located near the dipoles.

Concerning beam diagnostics four measuring positions (indicated as ML* in Fig. 1) are foreseen, with Faraday Cups, variable slits, beam profile grids and a beam transformer.

Note that, as DL1 and DL2 are the only dipoles in the low energy part, the dispersion vector (D,D') will keep os-

cillating in the RFQ and in the IH preserving the invariant:

$$\varepsilon_D = \left[D^2 + (\alpha(z)D + \beta(z)D')^2 \right] /\beta(z) \qquad (2)$$

where $\alpha(z)$ and $\beta(z)$ are the Twiss functions. This means that, if δ is the energy spread before the dipoles, $\varepsilon_D \delta^2$ is the corresponding contribution to the transverse emittance. It is easy to realize that ε_D depends upon the square of the resolution; indeed at the object point:

$$\varepsilon_D \approx \frac{D^2}{\beta} = 4\varepsilon\frac{D^2}{4\varepsilon\beta} = \frac{4\varepsilon}{R^2} \qquad (3)$$

For this reason a system like ours, with a high resolution and an intrinsically low acceptance in the accelerators, needs a high stability in the power supplies of the source and of the dipoles; the power supply of DL1 and DL2 has been specified with 10^{-5} stability.

4 PB RFQ

Downstream of the LEBT an RFQ structure accelerates the ion beam from 2.5 keV/u to 250 keV/u. This structure operates at 101.28 MHz and, because of this relatively low resonant frequency, it is of a "4 rods" type. The beam, delivered by the ECR source operating in the "afterglow mode", has a time structure of 400 μs pulses with a repetition rate of 10 Hz and consequently the RFQ has a duty cycle of the order of 1%.

Due to the low beam current intensity delivered by the ECR (below 1 mA), the space charge effects are negligible in the beam dynamics analysis. This consideration, combined with an extensive study of different kinds of bunching techniques, led to a novel design procedure [4] in which the structure is divided into six different logical sections. The result is a structure 2.5 m long, with a transverse acceptance of more than 0.8 mm mrad, operating with a surface electric field lower than twice the Kilpatrick limit (22.8 MV/m) and with a transmission larger than 90%.

An important parameter is the ratio ρ/r_0 between the transverse radius of curvature of the electrodes and the average aperture. This is usually in the range $0.75 \div 1.0$, where the smaller value gives a higher accelerating field, the bigger a lower multipole component in the field. In our design is has been possible to choose $\rho = r_0$.

The most important design characteristics of this "4 rods" structure are the fully symmetrical supports and the "vane like" cross section of the electrodes [5]. The first design choice gives a structure which has no electrical dipole moment in the beam region, as confirmed by numerical simulations and cold modelling of the cavity; the second one makes the alignment of the electrodes in the structure more reliable with the presence of a reference plane for each electrode and increases the electrodes rigidity too.

The geometry of the supports of the electrodes has been optimized with respect to the shunt impedance values and the final choice is to adopt some triangular supports.

5 MEBT

Both RFQ and IH work at the same frequency, but have a different transverse focussing structure. The first is a FODO with $\beta\lambda$ period; the second is a triplet-drift-triplet with $4\beta\lambda$ period. Moreover the bunches have to enter the IH longitudinally convergent.
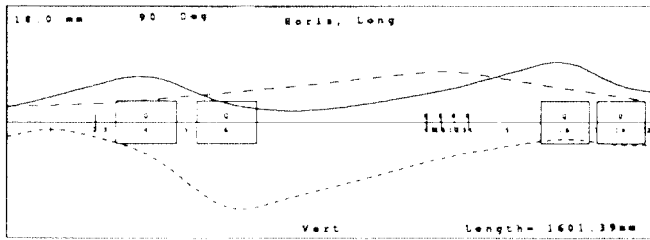
Figure 3: Beam envelopes in the MEBT

Therefore the beam matching in the MEBT is not "natural", and requires action on six independent machine parameters: the voltage and the position of a buncher and the field of four quadrupoles. The total length of the MEBT (1.6 m) has been kept as small as possible so to reduce the length of the pulse at the buncher ($\pm 44°$) and the consequent non linearity in the longitudinal phase-plane.

The buncher is a four-gap quarter wave resonator. This choice has been made so to have the maximum shunt impedance and to get the required voltage (≈ 100 kV) with the available rf-power.

In Fig. 3 are shown the envelopes of the beam in the MEBT.

6 BEAM PARAMETERS

In table 3 a consistent set of parameters is listed; according to simulations beam losses are concentrated in the RFQ in the bunching process. No significant emittance increase has been observed; nevertheless the emittance value used in the simulation of the RFQ dynamics (.5 mm mrad) has been assumed bigger than the output of the source (.35

mm mrad), while the acceptances do increase from one section to the next one. This gives a safety margin to cope with misalignments and mismatch of the source.

Table 3: Beam parameters

	LEBT	RFQ	MEBT		
Length	7.0	2.5		1.6	m
Acceptance	.46	.8		1.	mm mrad
Transmission	100	94		100	%
Energy	2.5	2.5	250	250	keV/u
ϵ	.35	.5	.5	.5	mm mrad
α_x	0	.8	-1.5	1.7	—
α_y	0	.8	1.2	.51	—
β_x	.025	.024	.23	.96	m
β_y	.025	.024	.24	.55	m
ϵ_l	—	—	32	35	$°$keV/u
β_l	—	—	3.3	6.2	$°$u/keV
$\Delta\varphi$	—	—	10	15	$°$
α_l	—	—	0	-1.55	—

7 ACKNOWLEDGMENTS

8 REFERENCES

[1] H.Wollnik, J.Brezina,C.Giesse, "GIOS A program for the Design of Ion Optical Systems", 2 Physidalisches Institut, Universität Geissen, Geissen (1987).

[2] N. Angert et al. "A new 1.4 MeV/u injector Linac for UNILAC", Proc. of the 1990 Linear Accelerator Conference, p.749.

[3] M. Bourgarel, private communications.

[4] G. Amendola, A. Pisent, J. Quesada, M. Weiss, "Beam Dynamics Studies for the CERN Lead-Ion RFQ", this Conf.

[5] A. Lombardi, G. Parisi, M. Vretenar, "Comparison study of RFQ Structures for the Lead Ion Linac at CERN", this Conf.